

Microcontroller-Based Model Design of Automatic Center of Gravity and Ballast Measurements for MK Bomb Series

Muhammad Zuhnir Piliang*, Agung Hirawan, and Rudi Lazuardi

Department of Physics, Republic Indonesia Defense University, Sentul-Bogor, West Java, Indonesia

*Corresponding Author: zuhnir.piliang@idu.ac.id

ARTICLE INFO

Article history:

Received 17 December 2024

Revised 11 March 2025

Accepted 04 April 2025

Available online 21 April 2025

E-ISSN: 2656-0755

P-ISSN: 2656-0747

How to cite:

M. Z. Piliang, A. Hirawan and R. Lazuardi " Microcontroller-Based Model Design of Automatic Center of Gravity and Ballast Measurements for MK Bomb Series," Journal of Technomaterial Physics, vol. 07, no. 01, pp. 51-62, Feb. 2025, doi: 10.32734/jottp.v7i1.19362.

ABSTRACT

The determination of center of gravity (CG) of Mark 80 series bomb is crucial before being released from fighter-aircraft to reduce or eliminate bomb-pitching; thus, improving target accuracy. Current CG measurement in the service remains conventional, takes a long time, so the determination of ballast is guesswork, and the equipment used is not integrated. Therefore, this study aims to design a model of a microcontroller-based CG and ballast measuring instrument. This tool model uses two load cell sensors (as scales) to measure the weight of the bomb and two ultrasonic sensors to measure the distance between scales. The interface is LCD as digital output, keypad as ballast control and Arduino mega. The experimental method in this study employed test objects in the form of miniature MK 81 bombs and bomb-like test objects with known CG. A total of 6 types of tests obtained a tool accuracy rate of 99.2% with an accuracy of 2 mm. Given the efficiency and accuracy of the measurement, this model of CG and ballast measuring instrument can be a smart solution for military agencies to be used as an effective CG measuring tool for MK 80 bombs.

Keywords: Center of Gravity, Ballast, MK Bomb, Microcontroller Design.

ABSTRAK

Penentuan pusat gravitasi (Center of Gravity/CG) pada bom seri Mark 80 sangat penting sebelum dilepaskan dari pesawat tempur untuk mengurangi atau menghilangkan *pitching* bom, sehingga meningkatkan akurasi sasaran. Metode pengukuran CG yang digunakan saat ini masih bersifat konvensional, memerlukan waktu yang lama, sehingga penentuan ballast dilakukan secara perkiraan, dan peralatan yang digunakan tidak terintegrasi. Oleh karena itu, penelitian ini bertujuan untuk merancang model alat ukur CG dan ballast berbasis mikrokontroler. Model alat ini menggunakan dua sensor load cell (sebagai timbangan) untuk mengukur berat bom dan dua sensor ultrasonik untuk mengukur jarak antara timbangan. Antarmuka yang digunakan mencakup LCD sebagai output digital, *keypad* sebagai kontrol ballast, dan Arduino Mega sebagai pengolah data. Metode eksperimen dalam penelitian ini menggunakan objek uji berupa miniatur bom MK 81 dan objek uji serupa bom dengan CG yang telah diketahui. Dari enam jenis pengujian yang dilakukan, alat ini memiliki tingkat akurasi sebesar 99,2% dengan ketepatan hingga 2 mm. Dengan efisiensi dan akurasi pengukuran yang tinggi, model alat ukur CG dan ballast ini dapat menjadi solusi cerdas bagi institusi militer sebagai alat pengukur CG yang efektif untuk bom MK 80.

Kata Kunci: Titik Berat, Balast, Bom MK, Rancangan Mikrokontroler.



This work is licensed under a Creative Commons Attribution-ShareAlike 4.0 International.
<http://doi.org/10.32734/jottp.v7i1.19362>

1. Introduction

The MK 81 bomb is a conventional, unguided bomb originally developed in the United States but now independently produced by Indonesia's defense industry[1]. During deployment in flight, excessive pitch, roll, and yaw movements in the MK 81 often disrupt the bomb's stability post-release from a combat

aircraft[2]. This instability presents several risks, including potential collisions with the aircraft's wings, inaccurate targeting on the ground, and failure to detonate if the bomb's fuze does not impact the ground due to tail-first landing. Addressing these challenges, A study modified the fin slot on the bomb's tail fins and added a roll tab to the aileron, aiming to reduce excessive pitch, roll, and yaw [3]. While the modifications successfully dampened roll and yaw movements, the pitch issue remained unresolved. In Priyono's subsequent study in 2012, it was identified that the bomb's center of gravity (CG) significantly influenced pitching motion [3]. To minimize this movement, CG recalculations were required for each bomb, even though the CG was already theoretically known. This recalibration was especially necessary for the mass production of MK 81 bombs, as well as for CG and ballast weight calculations post-production. However, CG calculations are currently time-consuming due to a conventional, trial-and-error approach in determining the required ballast weight.

Typically, CG measurements for bombs still rely on manual measuring tools and scales, which are large and require considerable physical effort to set up due to their lack of integration [4]. Additionally, reading variability introduced by the human factor increases measurement uncertainty. A common discrepancy exists between the CG position on the bomb's technical design and the CG after manufacture, necessitating repeated measurements to confirm the final CG position [5]. Discrepancies between theoretical CG and experimental (recalculated) CG mean the bomb must be modified by adding ballast weight to either the nose or tail to match the experimental CG to the theoretical CG [6]. This adjustment increases the overall weight, but the current ballast determination is manual and still based on the CG position. Therefore, accurately determining CG position and ballast weight is essential.

Currently, an efficient and practical method for CG and ballast determination remains unavailable. Observations indicate that CG was initially determined by suspending the MK-81 bomb body and balancing it to identify its midpoint. By 2004, it has been introduced a more structured approach by applying a center-of-gravity equation for two-dimensional CG calculations. This method involves using two scales, a measuring tape, and a water level. Before weighing, several setup steps are necessary: setting the distance between scales, balancing the scales with the water level, moving the bomb multiple times with a crane, and measuring each bomb component, with 20 minutes of a single measurement. The main drawbacks of this method include lengthy setup time, significant labor requirements, separated components, and the need for estimations in ballast weight determination [7]. Thus, this present study proposes the development of an automatic model for measuring center of gravity (CG) and ballast weight for MK 80 series bombs using a microcontroller. This system aims to streamline CG and ballast measurement for MK-81 and MK-82 bombs, making the process more efficient and user-friendly.

2. Research Methodologies

2.1. Model Design and Instrumentation

This study employs a quantitative approach to evaluate the effectiveness of a center of gravity (CG) and ballast weight measurement model. The developed CG measurement model mimics the operational principles of an actual CG measuring tool used for MK-80 series bombs but is scaled for small test objects in this study. The CG measurement model design is shown in Figure 1. Key components include:

1. Two Load Cell Sensors: Measure the object's weight.
2. Two Ultrasonic Sensors: Measure distance.
3. Keypad: Allows input of bomb dimensions.
4. LCD 16x2 Display: Outputs CG and ballast data.
5. Arduino ATmega Microcontroller: Serves as the primary processing unit, integrating weight and distance inputs to calculate CG.

Each component is interconnected, allowing the model to detect and display data such as weight and spatial measurements as detected by the sensors.

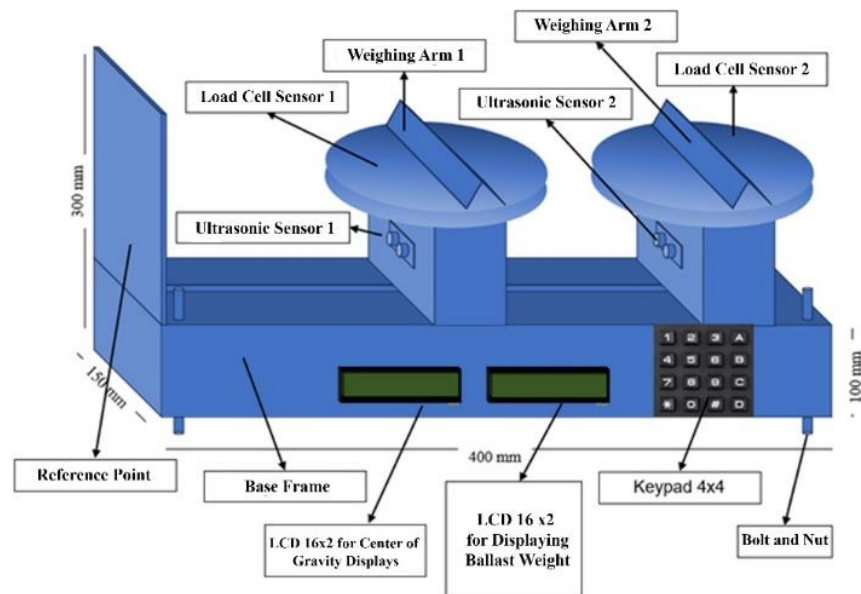


Figure 1. Measurement model design in center of gravity determination

2.2. Model Design and Instrumentation

The instrument operates based on rigid body CG calculation principles, where the CG is derived by dividing the total moment of position and mass variables by the total detected mass at specific points, as illustrated in Figure 2.

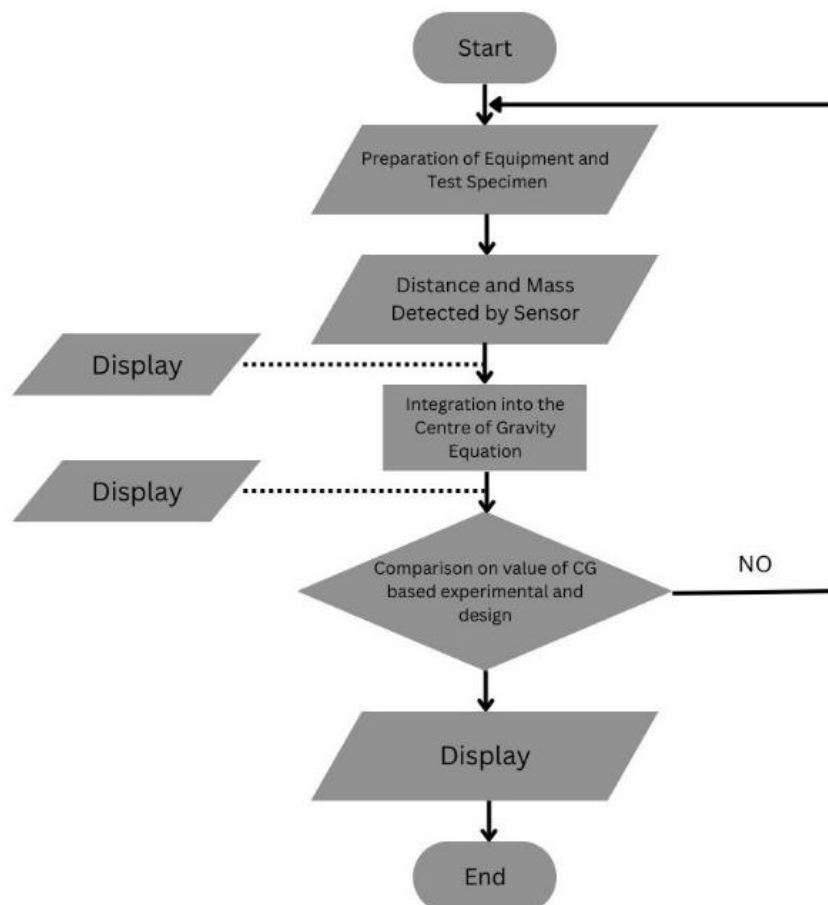


Figure 2. Flowchart of CG calculations

In this study, CG calculations focus on the x-axis, reflecting the non-uniform geometry of the bomb along this axis, as shown in Figure 3.

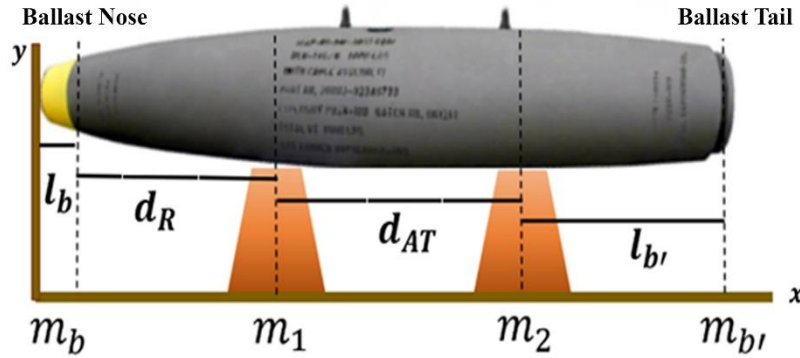


Figure 3. Model of mechanics calculations on homogenous rigid body

2.3. CG Calculation on the x-axis

The CG on the x-axis is calculated as Equation (1)

$$x_{CG} = \frac{(x_1 \cdot w_1) + (x_2 \cdot w_2) + \dots}{w_1 + w_2 + \dots} \quad (1)$$

Where x_{CG} is the center of gravity along the x-axis, x represents positions, and w denotes weights at specified points.

2.4. Ballast Calculation for CG Adjustment

Figure 4 illustrates the CG analysis for the MK 81 bomb model, adapted to small-scale tests. Equation (1) calculates CG along the x-axis, while Equations (2) and (3) estimate ballast weight based on theoretical CG adjustments:

1. Ballast Weight at Nose (Equation 2)

$$m_b = \frac{(l_b + d_R) \cdot m_1 + (l_b + d_R + d_{AT}) \cdot m_2 - x_{CG,t} \cdot (m_1 + m_2)}{x_{CG,t} - l_b} \quad (2)$$

2. Ballast Weight at Tail (Equation 3)

$$m_{b\prime} = \frac{(l_{b\prime} + d_R) \cdot m_1 + (l_{b\prime} + d_R + d_{AT}) \cdot m_2 - x_{CG,t} \cdot (m_1 + m_2)}{x_{CG,t} - l_{b\prime}} \quad (3)$$

where $x_{CG,t}$ represents theoretical CG; l_b and $l_{b\prime}$ denote ballast positions at the nose and tail, respectively.

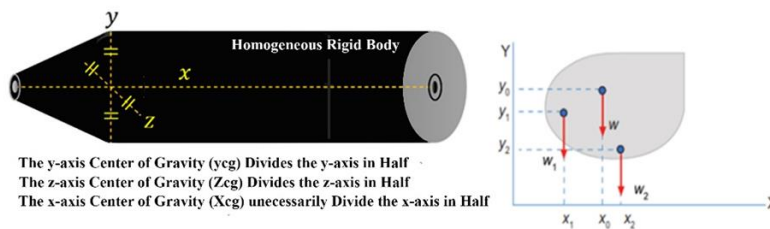


Figure 4. CG Analysis of MK 81 bomb model

2.5. Testing Procedures

Test 1 – CG Measurement Flexibility

- Tested on a hollow cylindrical object (PVC pipe, 600 mm length, 60 mm diameter, 207.8 g weight).
- Variations included altering distances between scales (d_{AT}) and reference points (d_R) to assess the flexibility of the model for different component positions.

Test 2 – Object Shape Consistency

- CG measurement was conducted on six test objects, including an MK-81 bomb model and five hollow, asymmetrical cylinders.
- The goal was to evaluate the model's consistency and accuracy across different shapes similar to the MK 80 series.

Test 3 – Ballast Weight Determination

- Performed on a symmetric hollow cylinder (600 mm length, 60 mm diameter, 207.8 g weight, $x_{CG,t} = 298$ mm).
- A disruptive weight (plasticine) was added at 100 mm from one side to shift the CG.
- Ballast was then added to the opposite side to return the CG to its original position.

Each test provided insights into the model's accuracy, flexibility, and effectiveness in determining the CG and ballast of MK-81 and MK-82 bomb models.

In this study, d_R represents the distance from the reference point to Scale 1, and d_{AT} denotes the distance between the two scales. The masses measured at Scale 1 and Scale 2 are represented as m_1 and m_2 , respectively. To determine the required ballast weight for CG adjustment, Eq. 1 was modified, assuming three main mass support points along the bomb's structure. The ballast was examined at two points—the bomb's nose and tail—denoted as m_b for the nose ballast mass and m_b' for the tail ballast mass, shown in Equation (3).

2.6. Experimental Testing Procedures

To evaluate the system's effectiveness, three tests were conducted to analyze the influence of different variables. The first test examined the effect of varying the distance between scales (d_{AT}) and the reference point (d_R) on the device's accuracy in measuring the center of gravity (CG). The second test assessed how variations in the shape of the test object influenced CG measurement accuracy. Finally, the third test evaluated the device's ability to determine the ballast weight needed to stabilize the CG. In the first test, the CG position $x_{CG,t}$ of a hollow cylindrical object was measured to assess the flexibility of the CG measurement device with varying positions of components. The test object was a PVC pipe with a length of 600 mm, diameter of 60 mm, and weight of 207.8 g. A combination of variations in d_{AT} and d_R was applied[8].

The second test involved measuring the CG position $x_{CG,t}$ of six solid objects resembling the shape of a bomb to assess the device's accuracy and consistency in measuring objects with similar dimensions. Although the device was designed for MK 81 and MK 82 bombs, its flexibility was tested to determine if it could measure other bomb types, provided they resemble the MK 80 bomb series. The test objects included an MK 81 bomb model, one symmetric hollow cylinder (filter), and four asymmetric hollow cylinders (glass bottles of varying shapes), as shown in Figure 5.

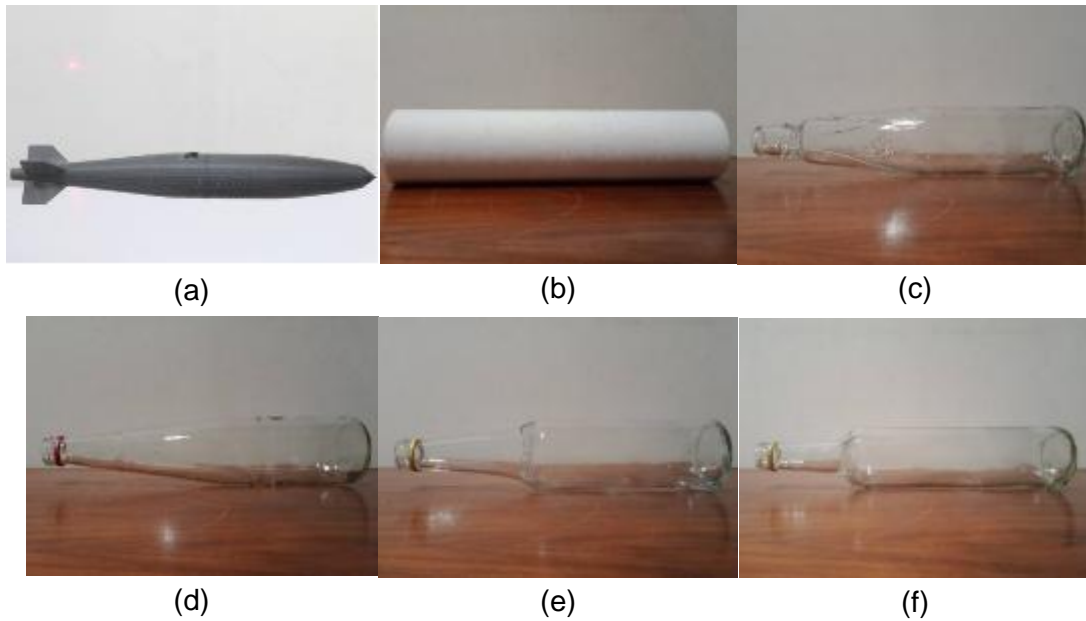


Figure 5. Geometrical shapes of testing model: (a) MK81 bomb model, (b) Symmetric hollow cylinder (filter), (c) Asymmetric hollow cylinders (bottle 1), (d) Asymmetric hollow cylinders (bottle 2), (e) Asymmetric hollow cylinders (bottle 3), (f) Asymmetric hollow cylinders (bottle 4).

In the third test, the device's ability to calculate the necessary ballast weight required to adjust the CG of a symmetric hollow cylinder (PVC pipe with length 600 mm, diameter 60 mm, weight 207.8 g, and $x_{CG,t}=298$ mm) was evaluated. A disruptive weight, made from plasticine, was added 100 mm from one end to shift the CG toward that end. A ballast weight was then added to the opposite end to return the CG to its original position at 298 mm.

Upon completing testing and data collection, several analyses were conducted to verify the validity and reliability of the test data, including linear regression analysis, measurement error, measurement uncertainty, accuracy, and precision. Linear regression was used to analyze the causal relationship between variables on a linear graph (LFD ITB, n.d.). The regression equation is expressed as Equation (4).

$$Y = a + b(x) \quad (4)$$

where Y is the dependent variable, x is the independent variable, a is the constant, and b is the regression coefficient. This equation can be generated in Microsoft Excel through linear regression plotting. In this study, Y represents the experimental CG position $x_{CG,t}$ while x includes variables such as m_1 , m_2 , dAT and dR . Additionally, a determination coefficient (R^2) was calculated to measure the relationship between the independent and dependent variables (Wijaya, 2011), with values interpreted as follows: 0.00 – 0.199: Very low correlation; 0.20 – 0.399: Low correlation; 0.40 – 0.599: Moderate correlation; 0.60 – 0.799: Strong correlation; 0.80 – 1.000: Very strong correlation.

Measurement error, or the percentage error, quantifies the degree of inaccuracy in measurements and is calculated as Equation (5).

$$\%E = \left(\left| \frac{x-x'}{x'} \right| \times 100\% \right) \quad (5)$$

While the precision of the designed measurements aims to observe the consistency in cycles of measurements. Thus, the precision percentage is calculated as Equation (6)

$$Precision = 100\% = \left(\left(1 - \left| \frac{x_n - \bar{x}}{\bar{x}} \right| \right) \times 100\% \right) \quad (6)$$

As the X_n = the order of measurements results, and \bar{x} = the average of measurements. The results were then used as classification basis to determine the precise features of the designed measurements, as (1) precision when $<0.5\%$, (2) working if $\pm 1-2\%$, and (3) rough gauge when $>3\%$.

3. Results and Discussion

3.1. Sensor Sensitivity Test (Calibration)

Before conducting the experiments, it is essential to calibrate the device to evaluate the measurement accuracy of each sensor. The calibration process employed an optical bench test specimen in the form of a block measuring 400 x 150 mm, with additional iron weights whose positions could be varied on the specimen. The setup of the equipment and test specimen during the calibration process is shown in Figure

6.

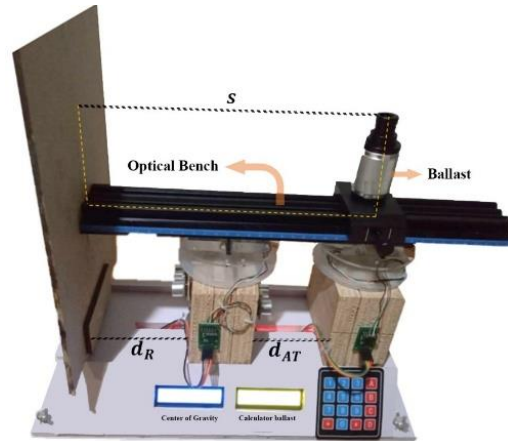


Figure 6. Calibration set up

After calibration, 24 test data points were obtained, as presented in Table 1

Table 1. Calibration data test

| No | s (mm) | $x_{CG,t}$ (mm) | $x_{CG,e}$ (mm) | $E(\%)$ | Accuracy (%) |
|---------|----------|-----------------|-----------------|---------|--------------|
| 1 | 24 | 162.47 | 163.89 | 0.87 | 99.16 |
| 2 | 39 | 165.67 | 170.80 | 3.10 | 96.90 |
| 3 | 54 | 168.78 | 170.67 | 1.12 | 98.88 |
| 4 | 69 | 171.91 | 173.70 | 1.04 | 98.96 |
| 5 | 84 | 174.98 | 177.30 | 1.32 | 98.68 |
| 6 | 99 | 178.12 | 179.42 | 0.73 | 99.27 |
| 7 | 114 | 181.27 | 183.43 | 1.19 | 98.81 |
| 8 | 129 | 184.39 | 187.03 | 1.43 | 98.57 |
| 9 | 144 | 187.57 | 189.91 | 1.25 | 98.75 |
| 10 | 159 | 190.62 | 193.14 | 1.32 | 98.68 |
| 11 | 174 | 193.64 | 195.00 | 0.70 | 99.30 |
| 12 | 189 | 196.88 | 201.19 | 2.19 | 97.81 |
| 13 | 204 | 199.99 | 202.80 | 1.40 | 98.60 |
| 14 | 219 | 203.08 | 206.69 | 1.78 | 98.22 |
| 15 | 234 | 206.24 | 209.90 | 1.77 | 98.23 |
| 16 | 249 | 209.34 | 213.23 | 1.86 | 98.14 |
| 17 | 264 | 212.44 | 216.50 | 1.91 | 98.09 |
| 18 | 279 | 215.58 | 219.76 | 1.94 | 98.06 |
| 19 | 294 | 218.71 | 223.09 | 2.00 | 98.00 |
| 20 | 309 | 221.86 | 225.64 | 1.70 | 98.29 |
| 21 | 324 | 224.94 | 229.76 | 2.14 | 97.86 |
| 22 | 339 | 228.07 | 230.60 | 1.11 | 98.89 |
| 23 | 354 | 231.16 | 235.33 | 1.80 | 98.20 |
| 24 | 369 | 234.23 | 237.00 | 1.18 | 98.82 |
| Average | | | | 1.54 | 98.47 |

s : Distance of the iron weight placement (mm); $x_{CG,t}$: Theoretical center of gravity (mm); $x_{CG,e}$: Experimental center of gravity (mm); E : Measurement error (%)

Based on the test data in Table 1, it was observed that the second trial had the highest error value at 3.1%, with the weight placed at a distance of 39 mm from the test specimen's reference point. Conversely, the 11th trial showed the smallest error value at 0.7%, with the weight located 174 mm from the reference point. These results indicate that the experimental value ($x_{CG,e}$) closely approaches the theoretical value ($x_{CG,t}$) as the weight moves closer to the midpoint of the test specimen. This trend is due to the decreasing influence of weight on the equilibrium of the test specimen's weight. This shows the importance of weight placement, especially in obtaining balance and equilibrium. In designing the measurement tools, there are three importance of accurate weight placement, including postural balance and health [9], weight distribution platforms [10], and gravitational configuration effect [11]. Figure 7 presents a graph illustrating the relationship between $x_{CG,e}$ and the variation in weight distance.

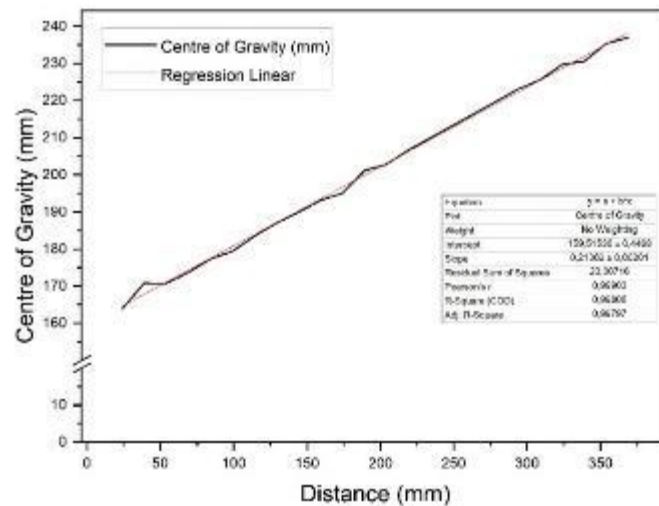


Figure 7. Calibration results on measurements

From 24 calibration trials, the average measurement error of the instrument was 1.5%, indicating a high level of accuracy. This is supported by the coefficient of determination (R^2) shown in the graph (Figure 7), which has a value of 0.9981. This demonstrates that the experimental center of gravity values $x_{CG,e}$ align linearly with variations in weight placement distance, resulting in a strong measurement accuracy of 98.5%. The accuracy is attributed to the close match between the test object's length and the instrument's length, as well as the object's mass being within the instrument's weighing capacity.

3.2. Testing x_{CG} on Hollow Cylindrical objects Through Variations in Distance Between Scales (d_{AT}) and Reference Points (d_R)

Table 2. Measurements data of on a pipe with variations in scale distances and reference points

| Trials | d_{AT} (mm) | d_R (mm) | $x_{CG,e}$ (mm) | $x_{CG,t}$ (mm) | $E(\%)$ | Accuraction (%) | Precision (%) |
|---------|------------------|---------------|--------------------|--------------------|---------|--------------------|------------------|
| 1 | 105 | 200 | 298.93 | 297.42 | 0.51 | 99.49 | 1.39 |
| 2 | 120 | 210 | 297.86 | 297.83 | 0.01 | 99.99 | 1.03 |
| 3 | 135 | 220 | 296.07 | 299.52 | 1.15 | 98.85 | 0.42 |
| 4 | 150 | 230 | 294.97 | 297.06 | 0.70 | 99.30 | 0.05 |
| 5 | 165 | 240 | 294.54 | 299.20 | 1.56 | 98.44 | 0.09 |
| 6 | 180 | 250 | 294.53 | 299.72 | 1.73 | 98.27 | 0.10 |
| 7 | 195 | 260 | 293.79 | 299.13 | 1.78 | 98.21 | 0.35 |
| 8 | 210 | 270 | 293.41 | 298.10 | 1.57 | 98.43 | 0.48 |
| 9 | 225 | 280 | 292.76 | 298.05 | 1.77 | 98.22 | 0.70 |
| 10 | 240 | 290 | 291.33 | 297.28 | 2.00 | 98.00 | 1.18 |
| Average | | | (294.82 ± 0.72) | | 1.28 | 98.72 | 0.58 |

In this experiment, 10 variations of reference point distance (d_R) and 10 variations of distance between scales (d_{AT}) were applied in a paired manner. The variations were adjusted to the device dimensions, with d_{AT} shifted by 15 mm and d_R shifted by 10 mm for each variation. The trials began with a pair of $d_{AT} = 105$ mm and $d_R = 200$ mm; followed by $d_{AT} = 120$ mm and $d_R = 210$ mm; continued up to $d_{AT} = 240$ mm and $d_R = 290$ mm. The measurements result of x_{COG} obtained automatically through the variations of d_{AT} and d_R , are shown in Table 2.

The mean experimental center of gravity ($\bar{x}_{CG,e}$) was found to be 294.82 mm with a measurement error of 1.28%. This confirms the instrument's accuracy and precision, with a measurement uncertainty of ± 0.72 mm. Expressed with significant figures, the result is (295 ± 0.72) mm. The instrument's effectiveness is reflected by its high accuracy (98.72%) and precision (0.58%), categorizing it as a functional measuring tool. However, as observed in Table 2, a pattern emerges in the relationship between $x_{CG,e}$ and measurement errors. As the distances d_R (reference point) and d_{AT} (distance between scales) increase, the discrepancy between $x_{CG,e}$ and theoretical centre of gravity values $x_{COG,t}$ grows, leading to larger errors. For instance, the smallest error (0.01%) was recorded when $d_R = 210$ mm and $d_{AT} = 120$ mm, indicating these are the optimal settings for accurate center of gravity measurements. Systematic errors, such as misalignment of the reference point and scale during adjustments, contribute to the inaccuracies. Ensuring a perpendicular orientation between the distance sensor and the reference plane is essential for optimal ultrasonic signal reception by the sensor's receiver.

3.3. Effect of Object Shape on Measurement Accuracy

In a separate test, objects of varying shapes were repeatedly measured ($n=10$) under constant d_{AT} and d_R constant. The results, summarized in Table 3, demonstrate the instrument's consistency in measuring center of gravity across different test objects. The average measurement error across all objects was 0.83%, confirming both accuracy and precision. The tool achieved an overall accuracy of 99.17% and precision of 0.27%, categorizing it as a precise instrument.

Table 3. Recorded data of atom bomb models

| Geometrical Models | Dimension | | $\bar{x}_{CG,e}$ (mm) | $\bar{x}_{CG,t}$ (mm) | \bar{E} (%) | Accuracy (%) | Precision (%) |
|--------------------|-------------|------------|--------------------------|--------------------------|------------------|-----------------|------------------|
| | l (mm) | m (g) | | | | | |
| A | 345 | 71.00 | 160.66 | 161.25 | 0.50 | 99.63 | 0.50 |
| B | 250 | 119.8 | 127.44 | 128.00 | 0.49 | 99.51 | 0.39 |
| C | 275 | 307.2 | 160.87 | 161.21 | 0.33 | 99.67 | 0.37 |
| D | 285 | 337.6 | 178.47 | 175.29 | 1.81 | 98.19 | 0.22 |
| E | 280 | 320.1 | 169.40 | 170.62 | 0.71 | 99.29 | 0.08 |
| F | 285 | 353.5 | 168.16 | 170.11 | 1.15 | 98.85 | 0.05 |
| Average | | | | | 0.83 | 99.19 | 0.27 |

Comparison with previous results (Table 2) reveals differences in precision when testing a PVC pipe (hollow cylinder) versus bomb-like test objects (symmetric and asymmetric hollow cylinders). The PVC pipe tests, which involved combined distance variations, yielded a precision of 0.57%, classifying the tool as functional. Conversely, the bomb-like objects achieved higher precision (0.27%), classifying the instrument as precise.

These differences stem from the varying dimensions of the test objects. The PVC pipe, with a length of 600 mm and diameter of 60 mm, exceeded the instrument's length (400 mm) and had a mass of 207.8 g. In contrast, the bomb-like objects were smaller (250–345 mm length, 71–337.6 g mass). The shorter test objects allowed for better sensitivity of the ultrasonic sensor (HCSR04), as the ultrasonic wave reflections were more effectively captured at shorter (d_R) distances. This highlights the importance of object dimensions in maintaining the instrument's accuracy and precision. Also, tools designed for weight balance, including mechanisms for automatic loading and precise positioning of weights would achieve accurate weight distribution during measurements [12].

3.4. Effect of Disruptive Weight Variations on the Device's Ability to Determine Ballast Weight

In this test, the position of the ballast was arbitrarily set at 100 mm from one end of the test object or 500 mm from the opposite end. The disruptive weight was varied across 10 trials with increments of 10 grams,

resulting in weights of 10, 20, 30, 40, 50, 60, 70, 80, 90, and 100 grams. The results are summarized in Table 4.

Table 4. Ballast test results

| Trials | Weight (g) | m_{be} (g) | m_{bt} (g) | E (%) | Accuracy (%) |
|---------|------------|--------------|--------------|---------|--------------|
| 1 | 10 | 7.40 | 6.60 | 12.12 | 87.88 |
| 2 | 20 | 15.00 | 13.80 | 8.69 | 91.30 |
| 3 | 30 | 18.10 | 17.40 | 4.02 | 95.98 |
| 4 | 40 | 26.30 | 25.10 | 4.78 | 95.22 |
| 5 | 50 | 32.10 | 31.10 | 3.21 | 96.78 |
| 6 | 60 | 38.00 | 37.10 | 2.42 | 97.57 |
| 7 | 70 | 40.80 | 40.00 | 2.00 | 98.00 |
| 8 | 80 | 47.20 | 46.50 | 1.50 | 98.49 |
| 9 | 90 | 51.70 | 51.30 | 0.78 | 99.22 |
| 10 | 100 | 57.10 | 57.30 | 0.35 | 99.65 |
| Average | | | | 3.99 | 96.01 |

m_{be} = Experimental ballast mass (g); m_{bt} = Theoretical ballast mass (g);
and E = Measurement error (%)

From Table 4, the first trial exhibited the largest measurement error at 12.12%, corresponding to a 10-gram disruptive weight. Measurement errors decreased below 5% starting from the third trial, where the disruptive weight was 30 grams. The smallest error, 0.35%, was recorded in the final trial with a 100-gram disruptive weight. As the disruptive weight increased, the measurement error consistently decreased. This trend suggests that there is a threshold below which the difference between the theoretical CG ($x_{CG,t}$) and experimental CG ($x_{CG,e}$) cannot be accurately measured due to the device's sensitivity limitations. Referring to Table 4, the device demonstrated its lowest accuracy, 87.88%, in the first trial, where $x_{CG,e}$ was 304.1 mm, deviating by 6.1 mm from $x_{CG,t}$. By contrast, in the fourth trial, an accuracy of 95.22% was achieved with an error of 4.78%, where $x_{CG,e}$ was 317.7 mm, deviating by 20 mm from $x_{CG,t}$.

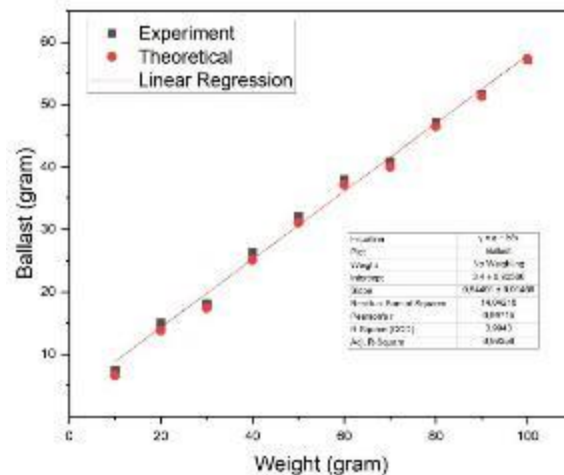


Figure 8. Comparative analysis of measurements and theoretical data

Based on the error and sensitivity analysis, the device was determined to achieve accuracies above 95% only when the difference between $x_{CG,t}$ and $x_{CG,e}$ exceeded 20 mm (2 cm). Differences below this threshold cannot be accurately measured by the device for test objects of 600 mm in length and 208.3 g in weight. The relationship between the ballast test results with the test objects is displayed in Figure 8 below. Across 10 trials, the average measurement error was 3.9%, indicating that the device performed optimally. The accuracy of the measurements is further supported by the correlation coefficient (R^2) value of 0.9943, demonstrating a strong linear relationship between the ballast mass ($m_{b,e}$) and the disruptive weight variations. Overall, the measurement data exhibited excellent accuracy, with an average accuracy of 96%.

Ballast mass is a dependent variable directly influenced by the disruptive weight variations. As the disruptive weight on the test object (representing an MK 81 bomb model) increases, the ballast mass required to maintain the center of gravity also increases proportionally. The need for ballast mass arises when there is a shift in the center of gravity due to uneven weight distribution. This is similar to the concept of added mass in fluid dynamics, where the mass of fluid moving with a body affects its dynamics, as seen in ship hulls [13]. In practical terms, the disruptive weight simulates excess or uneven material on one side of the bomb, which causes a shift in the CG from its intended design [14]. This issue often arises from production errors, such as material shortages, excess material, or uneven distribution during the casting process. An illustration of ballast addition due to disruptive weight can be seen in Figure 9.

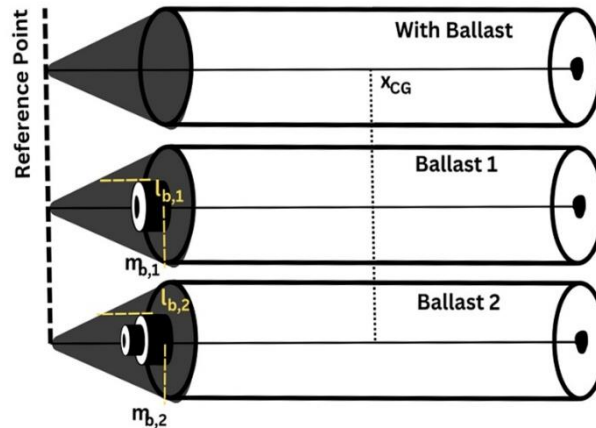


Figure 9. Schematic illustration of ballast addition

4. Conclusion.

A center of gravity (CG) measurement device for bombs has been successfully developed and functions effectively. The findings from this study demonstrate several aspects of the device's effectiveness, based on the position and distance between scales (d_{AT}) and the reference point (d_R) that significantly affect the CG measurement accuracy (longer distance, higher measurements errors). From the tests conducted with variations in d_{AT} and d_R the device achieved an accuracy of 98.72%, a precision of 0.58%, and a measurement uncertainty of 2 mm per measurement. Meanwhile, shape variations (symmetrical and regular dimensions) did not affect the CG of an object, shown from trial results with an accuracy of 99.12% and a precision of 0.27%. Due to the limitations of the sensors used, the device's accuracy decreases when the length of the test object exceeds the device's maximum capacity (<10kg). Variations in the disruptive weight significantly influenced the ballast mass of the test object, subsequently; the heavier ballast is required to restore the CG position to its theoretical value. The trial results showed an accuracy of 96% for ballast tests, effective ballast adjustment occurs when the difference between $x_{CG,e}$ and $x_{CG,t}$ exceeds 20 mm.

References

- [1] B. Pamungkas, "MK82 High Drag Bomb Parachute: Bom Spesialis Penghancur Sasaran Tertutup dan Sulit," *INDOMILITER*.
- [2] R. Mantri, V. Raghav, B. Koukol, N. Komerath, and M. Smith, "Study of Factors Driving Pitch, Roll, and Yaw Coupling in Bluff Body Aerodynamics," in *41st AIAA Fluid Dynamics Conference and Exhibit*, Reston, Virginia: American Institute of Aeronautics and Astronautics, Jun. 2011. doi: 10.2514/6.2011-3445.
- [3] E. Priyono, "Potensi Kemandirian Pembuatan Bom Tajam (Live Bomb) Di Dalam Negeri Untuk Mengatasi Embargo," *INDEPT*, vol. 2, no. 2, 2012.
- [4] S. Mandić, M. Pavić, B. Pavković, M. Ignjatović, and G. Ocokoljić, "Aerodynamic interceptors efficiency for subsonic missiles roll attitude control," *Scientific Technical Review*, vol. 67, no. 2, pp. 37–46, 2017. doi: 10.5937/str1702037M.
- [5] X. Zhao, Y. Yuan, Y. Dong, and R. Zhao, "Optimization approach to the aircraft weight and balance problem with the centre of gravity envelope constraints," *IET Intelligent Transport Systems*, vol. 15, no. 10, pp. 1269–1286, Oct. 2021. doi: 10.1049/itr2.12096.
- [6] Y. Miura, S. Nakanishi, E. Higuchi, K. Takamasu, M. Abe, and O. Sato, "Comparative evaluation of estimation of step gauge measurement uncertainty via Monte Carlo simulation," *Precision*

- Engineering*, vol. 55, pp. 390–396, Jan. 2019. doi: 10.1016/j.precisioneng.2018.10.007.
- [7] L. Liu, F. Zhu, J. Chen, Y. Ma, and Y. Tu, “A quality control method for complex product selective assembly processes,” *International Journal of Production Research*, vol. 51, no. 18, pp. 5437–5449, Sep. 2013. doi: 10.1080/00207543.2013.776187.
 - [8] F. Thiébaud, C. Lacroix, L. Andolfatto, and C. Lartigue, “Evaluation of the shape deviation of non rigid parts from optical measurements,” *The International Journal of Advanced Manufacturing Technology*, vol. 88, no. 5–8, pp. 1937–1944, Feb. 2017. doi: 10.1007/s00170-016-8899-3.
 - [9] D. Cotoros, C. Druga, I. Serban, and A. Stanciu, “Analysis of Postural Imbalance Due to Handling Weights During Physical Activities,” in *Proceedings of the International Conference on Human Systems Engineering and Design*, 2019, pp. 29–34. doi: 10.1007/978-981-13-6207-1_5.
 - [10] G. Bosscher, A. Tomas, S. Roe, D. Marcellin-Little, and B. D. Lascelles, “Repeatability and accuracy testing of a weight distribution platform and comparison to a pressure sensitive walkway to assess static weight distribution,” *Veterinary and Comparative Orthopaedics and Traumatology*, vol. 30, no. 2, pp. 160–164, Dec. 2017. doi: 10.3415/VCOT-16-09-0128.
 - [11] H. E. Almer and H. F. Swift, “Gravitational configuration effect upon precision mass measurements,” *Review of Scientific Instruments*, vol. 46, no. 9, pp. 1174–1176, Sep. 1975. doi: 10.1063/1.1134431.
 - [12] R. Mahmud, A. J. Rasel, and M. A. Rahman, “Design, fabrication and experimental study of a single plane balancing machine,” in *AIP Conference Proceedings*, 2016, p. 060001. doi: 10.1063/1.4958442.
 - [13] H. Zeraatgar, A. Moghaddas, and K. Sadati, “Analysis of surge added mass of planing hulls by model experiment,” *Ships and Offshore Structures*, vol. 15, no. 3, pp. 310–317, Mar. 2020. doi: 10.1080/17445302.2019.1615705.
 - [14] A. Zenner and A. Kruger, “Shifty: A Weight-Shifting Dynamic Passive Haptic Proxy to Enhance Object Perception in Virtual Reality,” *IEEE Transactions on Visualization and Computer Graphics*, vol. 23, no. 4, pp. 1285–1294, Apr. 2017. doi: 10.1109/TVCG.2017.2656978.